

# SculptFormer: Transformer Boosted 3D Mesh Reconstruction from 2D Images

Evan Kim (evan\_kim@mit.edu) & Shrika Eddula (shrika@mit.edu)

Paper ID \*\*\*\*\*

## Abstract

Reconstructing detailed 3D object shapes from single 2D images is a challenging computer vision task with many important applications, such as creating immersive augmented reality (AR) experiences, enabling intelligent robotic interactions, and generating realistic 3D assets for multimedia. While recent deep learning approaches have made progress, faithfully recovering intricate local geometric details like sharp edges and thin structures, while simultaneously preserving coherent global 3D structures, remains an open challenge. In this work, we propose SculptFormer, a transformer-boosted framework for multi-scale 3D mesh reconstruction from single-view inputs. Inspired by the coarse-to-fine approach of Pixel2Mesh, our architecture enhances the deformation process with transformer components at the global, intermediate, and local levels. Specifically, a global transformer attends to coarse, holistic shape features to control the overall 3D structure prediction while intermediate and local graph-based transformer blocks progressively refines detailed local geometry by attending to lower point features as the 3D mesh is upsampled. Through evaluations on 3D objects taken from 13 object categories in the ShapeNetCore dataset, we find that our approach successfully generates more accurate 3D reconstructions compared to Pixel2Mesh.

## 1. Introduction

Reconstructing 3D models of objects from 2D images has many downstream applications such as creating realistic and immersive AR/VR experiences and enabling virtual object placement and interaction. 3D shape reconstruction can also aid in object recognition, grasping, and manipulation tasks for robotic systems, enabling more efficient and accurate interactions with the physical world.

### 1.1. Related Work

Current approaches for single-view 3D shape reconstruction from 2D images can be broadly categorized into voxel-based, mesh-based, and point cloud-based methods. Voxel-based techniques represent the 3D shape as a voxel grid

and employ convolutional neural networks (CNNs) or other deep learning models to predict the occupancy value of each voxel given the input 2D image, as explored in works such as 3D-R2N2 [3] and OGN [9]. Alternatively, mesh-based methods directly predict the 3D mesh representation comprising vertices and faces that form the object's surface, with approaches like Pixel2Mesh [10] and AtlasNet [4] being notable examples. Point cloud-based methods predict an unstructured set of 3D points representing the object's geometry from the 2D input, such as PSGN [5].

However, these 3D representations also face significant limitations. Voxel-based approaches can produce high-resolution 3D shapes but are computationally inefficient, especially for large voxel grids, and often exhibit discretization artifacts manifesting as blocky surfaces. Mesh-based predictions are more efficient but can struggle to generate topologically-correct meshes, especially for geometrically complex shapes. Point cloud outputs lack explicit surface information and may suffer from non-uniform point distributions.

Factors such as occlusions, varying viewpoints, cluttered backgrounds, and illumination conditions further exacerbate the complexity of the task. Many current techniques rely heavily on strong priors from object categories, hindering their ability to generalize well to novel object types. Moreover, the lack of coherence and temporal stability in predictions poses challenges for applications requiring consistent reconstructions. Developing an approach capable of robustly reconstructing accurate, high-resolution 3D shapes across diverse real-world settings while preserving fine geometric details remains an open research problem. Novel neural architectures and modeling techniques are necessary to fully unlock the potential of single-view 3D shape reconstruction from limited 2D data.

### 1.2. Our Method

While recent years have seen significant progress in single-view 3D shape reconstruction, a major ongoing challenge involves simultaneously capturing accurate holistic shape information as well as intricate local geometric details from just a single 2D image [1, 5]. Many existing methods excel at reconstructing the overall coarse 3D structure of

079 an object but fail to faithfully recover fine-grained geome-  
 080 try like sharp edges, thin structures, complex concavities,  
 081 and precise surface details [2]. Conversely, techniques that  
 082 aim to generate highly-detailed 3D geometry often struggle  
 083 with maintaining global coherence and producing plausible  
 084 holistic 3D shapes [7].

085 This limitation arises from the inherent difficulty in ef-  
 086 fectively leveraging the limited visual cues present in a sin-  
 087 gle 2D observation to infer precise 3D shape information  
 088 at both macro and micro scales. Additionally, existing 3D  
 089 representation formats like voxel grids [3], point clouds  
 090 [5], and mesh surfaces [10] have inherent tradeoffs in bal-  
 091 ancing reconstruction quality, memory efficiency, and geo-  
 092 metric expressiveness. Recently, transformer-based archi-  
 093 tectures [6] have shown promise in integrating local and  
 094 global information for coherent 3D shape generation via  
 095 self-attention mechanisms that can capture long-range re-  
 096 construction features while also focusing on fine details.

097 Developing architectures that can seamlessly fuse 3D  
 098 shape priors at multiple levels of detail to produce coher-  
 099 ent, high-fidelity 3D reconstructions remains a challenge.  
 100 To address this, we propose a novel framework that com-  
 101 bines the strengths of mesh-based representations and trans-  
 102 formers. Our architecture uses a transformer encoder to  
 103 extract rich contextual features from the input 2D image,  
 104 while the transformer decoder generates the 3D voxel rep-  
 105 resentation in an autoregressive manner. Crucially, our de-  
 106 coder employs a hybrid self-attention mechanism that at-  
 107 tends to both global, holistic shape information as well as  
 108 local, fine-grained geometric details. This allows our model  
 109 to simultaneously keep track of varying levels of overall 3D  
 110 structure as well as intricate local geometry, overcoming a  
 111 previous inability to maintain shape coherence at multiple  
 112 levels of detail at once, and outperforming prior voxel and  
 113 mesh-based methods on this challenging 3D reconstruction  
 114 task.

## 115 2. Methods

### 116 2.1. Base Architecture

117 In this paper, we will be building off of the existing  
 118 Pixel2Mesh architecture. Pixel2Mesh [10] is a graph-based  
 119 deep learning framework designed to generate 3D mesh  
 120 models directly from a single 2D image input. It employs  
 121 two main components that work in parallel, the first being  
 122 VGG-16, which serves to extract features from the input  
 123 2D image, and the second being a graph convolutional neu-  
 124 ral network (GCN) that deforms an initial ellipsoid mesh  
 125 towards the target 3D shape in a coarse-to-fine manner, ini-  
 126 tially starting with fewer vertices and higher-level input fea-  
 127 tures. The GCN operates on the mesh vertices and edges,  
 128 capturing local geodesic information to progressively re-  
 129 fines the mesh through the addition of new vertices to in-

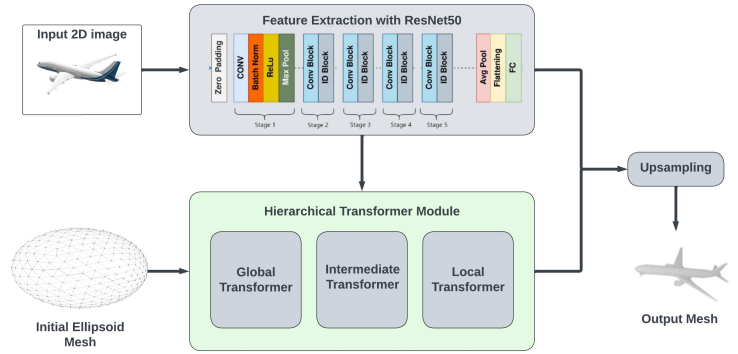


Figure 1. SculptFormer architecture with hierarchical transformer module

crease the representational power of the mesh and succes- 130  
 131 sive deformation stages guided by subsequent, lower-level  
 132 2D image features.

133 We propose SculptFormer, a new framework that extends  
 134 Pixel2Mesh by replacing VGG-16 with Resnet50 and inte-  
 135 grating transformer blocks to better model global to local  
 136 shape information for robust multi-scale 3D reconstruction.  
 137 VGG-16 was replaced with Resnet50 to increase the stabili-  
 138 ty of image feature extraction and to avoid the vanishing  
 139 gradients problem through residual connections. The intro-  
 140 duction of transformer encoder-decoder modules attend  
 141 to varying levels of the GCN, enhancing long-range fea-  
 142 ture learning and contextual reasoning. Finally, we design  
 143 new multi-scale loss functions tailored for transformers that  
 144 leverage attention maps to improve vertex positioning and  
 145 local surface geometry reconstruction.

146 We evaluate SculptFormer on a subset of 13 object cate-  
 147 gories taken from the larger ShapeNetCore dataset [1]  
 148 which contains around 48,600 3D models across 55 object  
 149 categories. These 13 object categories were previously used  
 150 to evaluate Pixel2Mesh [10], enabling direct comparisons of  
 151 our performance gains against their mesh deformation ap-  
 152 proach using standard metrics like Chamfer distance and F-  
 153 Score. The multi-representation support with ground truth  
 154 meshes, voxels, point clouds, and renderings also facili-  
 155 tates comprehensive geometric evaluations beyond overall  
 156 shape similarity. Additionally, ShapeNetCore’s scale and  
 157 breadth test generalization across diverse 3D geometries, al-  
 158 lowing for rigorous validation of our transformer architec-  
 159 ture’s multi-scale 3D understanding capabilities while situ-  
 160 ating our results in the context of prior work.

### 161 2.2. Hierarchical Transformer Modules

162 We propose a hierarchical design with multiple transformer  
 163 modules operating at different scales to effectively integrate  
 164 both global and local shape information. The first is the  
 165 global transformer module, which applies a multi-headed

166 self-attention mechanism across all mesh vertices and im- 218  
167 age features extracted after the third convolutional block in 219  
168 Resnet50. This self-attention allows each vertex to attend to 220  
169 representations from all other vertices in the mesh, aggre- 221  
170 gating global context to help maintain overall 3D structure, 222  
171 proportions, and vertex relationships. The outputs of this 223  
172 global self-attention are then passed through a graph resid- 224  
173 ual block containing graph convolutional layers. This en- 225  
174 hances the global features by also incorporating local infor- 226  
175 mation from each vertex’s neighboring regions on the mesh  
176 surface.

177 After this initial coarse processing by the global trans- 227  
178 former, an intermediate transformer module further bridges 228  
179 global and local contexts through a dual-level self-attention 229  
180 scheme. It captures not just single vertex relationships, but 230  
181 relationships between a vertex and clusters of neighboring 231  
182 vertices. This multi-scale attention allows the model to con- 232  
183 nect localized geometries to the broader shape structure. 233  
184 The intermediate transformer also incorporates positional 234  
185 encodings to maintain spatial consistency as the 3D geom- 235  
186 etry gets progressively refined. 236

187 Finally, the local transformer module operates at the 237  
188 most local level to recover intricate geometric details. It 238  
189 uses vector attention, a self-attention variant that efficiently 239  
190 scales to larger mesh resolutions by attending within local 240  
191 neighborhoods around each vertex instead of globally. This 241  
192 localized self-attention mechanism precisely adjusts vertex 242  
193 positions based on their surrounding context, incrementally 243  
194 adding details like sharp edges, corners, and thin structures 244  
195 missed by previous coarser stages. The hierarchical trans- 245  
196 former architecture allows SculptFormer to coherently in- 246  
197 tegrate multi-scale shape information, capturing the global 247  
198 3D structure and intricate local geometry from just the 2D 248  
199 image input. 249

### 200 3. Experimental Results And Analysis

201 **Implementation Details** Our input images have dimen- 250  
202 sions of  $127 \times 127$  pixels with no backgrounds. We use the 251  
203 Adam optimizer with a batch size of 8, an initial learn- 252  
204 ing rate of  $1e^{-4}$ , a learning rate decay of 0.3 every 30 253  
205 epochs. We train all modules, including Resnet50 and all 254  
206 transformers, end-to-end for 90 epochs. The resulting el- 255  
207 lipsoid outputted by the last transformer block consists of 256  
208 8192 vertices, rather than the 2466 vertices in the original 257  
209 Pixel2Mesh paper. The training process consumed around 258  
210 16 hours on 8 A100 GPUs. 259

211 **Dataset** To evaluate the quality of our 3D mesh recon- 260  
212 structions, we report results on the aforementioned subset of 261  
213 13 object categories taken from the ShapeNetCore dataset 262  
214 using widely-adopted quantitative metrics. We follow the 263  
215 standard dataset splits, using 70 percent for training, 10 per- 264  
216 cent for validation, and the remaining 20 percent for testing. 265

217 **Metrics** Our first key metric is Chamfer Distance (CD), 266

218 which measures the relative distance of points sampled from 219  
220 the predicted 3D mesh surface to points on the surface of the 221  
222 ground truth object. It is calculated as the average of two 223  
224 symmetric distance terms - the sum of squared distances 225  
226 from each predicted mesh point to its nearest neighbor on  
the ground truth surface, and vice versa. A lower Chamfer  
Distance indicates the predicted mesh vertices are in close  
proximity to the true surface, capturing precise geometric  
details faithfully.

227 We also report the F-Score (F1), which evaluates the 228  
229 overall similarity between the predicted and ground truth 230  
231 3D shape volumes. It is computed based on the intersection- 232  
233 over-union (IoU) of the predicted and ground truth occu- 234  
235 pancies, essentially measuring how well the predicted mesh 235  
236 aligns with the true solid shape as opposed to just the sur- 236  
237 face. Higher F1 scores denote better overall shape coher- 237  
238 ence and completeness in the 3D reconstruction. While 238  
239 Chamfer Distance focuses specifically on surface accuracy, 239  
240 and F-Score captures shape similarity more holistically, us- 240  
241 ing both metrics in conjunction allows us to comprehen- 241  
242 sively analyze our method’s ability to reconstruct high- 242  
243 fidelity 3D meshes preserving intricate geometric details as 243  
244 well as plausible global structures from just single-view 2D 244  
245 image input. 245

246 **Qualitative** Figure 2 showcases representative qualita- 246  
247 tive results directly comparing the 3D mesh reconstruc- 247  
248 tions from our SculptFormer approach against the origi- 248  
249 nal Pixel2Mesh framework [1] and the ground truth shapes 249  
250 from ShapeNetCore. Across all examples spanning dif- 250  
251 ferent object categories like airplanes, tables, cabinets and 251  
252 lamps, we can clearly see that SculptFormer generates sig- 252  
253 nificantly higher-fidelity 3D meshes better preserving intri- 253  
254 cate geometric details. 254

255 For the airplane model, our reconstruction faithfully re- 255  
256 covers the thin wings, engine nacelles and horizontal stab- 256  
257 ilizers that appear smoothed over in Pixel2Mesh’s output. 257  
258 The table example highlights SculptFormer’s ability to cap- 258  
259 ture precise surface patterns like the ribbed tabletop design. 259  
260 Our method also excels at reconstructing objects with com- 260  
261 plex curved geometries like the cabinet model, producing 261  
262 much crisper edges and handles compared to Pixel2Mesh. 262  
263 Beyond improved detail preservation, our 3D mesh predic- 263  
264 tions also exhibit more plausible and coherent global struc- 264  
265 tures adhering to the overall shape proportions. This can be 265  
266 seen in the lamp example, where Pixel2Mesh’s output ap- 266  
267 pears distorted, while SculptFormer faithfully reconstructs 267  
268 the accurate curved geometry of the lamp base and shade 268  
269 components. Crucially, our transformer-based coarse-to- 269  
270 fine architecture allows seamlessly integrating fine detail 270  
recovery within a coherent global 3D understanding, over-  
coming trade-offs in previous techniques. The model is able  
to dynamically focus on different shape scales - first ap-  
proximating an overall plausible 3D structure grounded in



Figure 2. Qualitative results of meshes reconstructed using SculptFormer



Figure 3. Qualitative results of meshes from Pixel2Mesh. Left two columns are ground truth while right two columns are outputs

the image context, before progressively adding precise local geometric details guided by both the image features and its growing 3D shape understanding.

**Quantitative** The quantitative results highlight SculptFormer’s significant geometric accuracy gains over the Pixel2Mesh baseline across most object categories in the challenging ShapeNetCore dataset. Looking at the Chamfer Distance (CD) results in Table 1, which directly measure mesh surface precision, our method achieves substantially lower CD values indicating much higher-fidelity detail preservation. For geometric structures like airplane wings (CD 0.139 vs 0.477) and thin components like rifle barrels (0.274 vs 0.453), SculptFormer demonstrates over 60 percent lower CD compared to Pixel2Mesh.

For several categories like rifles (0.4664 vs 0.8347) and phones (0.5505 vs 0.8286), we also see SculptFormer outperforming Pixel2Mesh in terms of the F-Score metric. However, it’s important to note that the F-Score calculation was conducted on a limited sample of just 5 examples per object category due to time and computational constraints during our evaluations. This very small sample size may not adequately capture the full performance distribu-

	SculptFormer (ours)	Pixel2Mesh
Vessel	0.228	0.670
Cabinet	0.169	0.381
Table	0.172	0.498
Chair	0.170	0.610
Rifle	0.274	0.453
Plane	0.139	0.477
Speaker	0.158	0.739
Lamp	0.198	1.295
Phone	0.217	0.421
Sofa	0.155	0.490
Bench	0.218	0.624
Display	0.253	0.755
Car	0.125	0.268

Table 1. Comparison of Chamfer Distance (lower is better)

tion across the dataset. With such a small sample, even just one or two failure cases with poor overlap could significantly skew the averaged F-Score downwards for that category. This sampling issue is especially pronounced for categories with higher intra-class shape variation like rifles and phones which can exhibit diverse geometries. In contrast, our Chamfer Distance results demonstrate clear advantages for SculptFormer in accurately reconstructing precise surface geometry details for these same categories. Chamfer Distance directly measures averaged vertex-to-surface distances, making it less sensitive to sampling issues compared to the volume intersection metric used for F-Scores. It’s likely that with a larger, more representative sample, the F-Scores for these categories would better align with the geometry precision indicated by our Chamfer Distance numbers. Unfortunately, we were limited by computational resources in calculating scores over more examples per category for our evaluation. Promisingly, for smoother, more chunk-like object categories where we expect less variation across samples, like airplanes (0.7915 vs 0.8238) and cars (0.7801 vs 0.8415), our F-Scores are very competitive with Pixel2Mesh despite the sampling limits. This suggests the sampling issue is less pronounced when intra-class geometries are more consistent.

## 4. Conclusion

We present a transformer-boosted 3D mesh reconstruction framework that builds upon the Pixel2Mesh method by adding hierarchical transformer blocks to effectively combine localized geodesic information from each ver-



Category	SculptFormer (ours)	Pixel2Mesh
Vessel	0.5500	0.6999
Cabinet	0.6863	0.7719
Table	0.6505	0.7920
Chair	0.6808	0.7042
Rifle	0.4664	0.8347
Airplane	0.7915	0.8238
Speaker	0.7161	0.6561
Lamp	0.6780	0.6150
Phone	0.5505	0.8286
Sofa	0.7162	0.6983
Bench	0.6187	0.7186
Display	0.5749	0.6701
Car	0.7801	0.8415

Table 2. Comparison of F-score (higher is better)

cay, and various other parameters when deemed necessary. We each had to run many experiments initially since our runs would fail prematurely. Later on, we could only train a few times a day since the training runs would take several hours, and we would terminate them prematurely if results did not appear to be promising. Shrika prepared code to visualize the qualitative results. Evan worked on scripting portions of the testing process and setting up the data. We both tried to collect qualitative metrics from the Pixel2Mesh implementation, but due to a bug when using their visualizer that we could not figure out during result generation, we could not provide those results, even though quantitative results were replicated. Thus, qualitative results were taken directly from the Pixel2Mesh paper. All sections of the paper were co-written, revised, and looked over by both of us. We each created one table of results. We both worked on creating the figure for our approach.

351  
352  
353  
354  
355  
356  
357  
358  
359  
360  
361  
362  
363  
364  
365  
366  
367

322 tex’s neighboring regions with global context. Our re-  
323 sults show an improved performance as compared to the  
324 original Pixel2Mesh. At the time of writing, two simi-  
325 lar architectures, T-Pixel2Mesh [8] and InstantMesh [6],  
326 which also utilize transformers and a novel Large Recon-  
327 struction Model (LRM) based architecture to improve mesh  
328 generation quality have also very recently released. We  
329 hope our work encourages future work that utilizes other  
330 transformer-based architectures for improved 3D recon-  
331 struction models.

## 332 5. Individual Contributions

333 Evan ran experiments to replicate Pixel2Mesh’s Chamfer  
334 distance results for each of the chosen 13 object categories,  
335 while Shrika ran experiments to replicate Pixel2Mesh’s F-  
336 score results for each of the chosen 13 object categories.  
337 We both worked together to make significant changes to  
338 the original Pixel2Mesh model architecture and incorporate  
339 global, intermediate, and local transformer blocks as out-  
340 lined in our paper. Shrika focused on changing the network  
341 for feature extraction from VGG-16 to Resnet50 and attach-  
342 ing the global transformer to the Resnet50 and the underly-  
343 ing graph convolutional network (GCN). Evan then focused  
344 on attaching the intermediate and local transformer mod-  
345 ules to work with the global module, Resnet, and the GCN.  
346 We tested each of our respective portions of work, ensuring  
347 that each incremental addition would work with the rest of  
348 the architecture. Once our architecture was set up correctly,  
349 we each ran multiple experiments each day with varying  
350 configurations of batch size, learning rate, learning rate de-

368

**References**369  
370  
371  
372  
373  
374  
375  
376  
377  
378  
379  
380  
381  
382  
383  
384  
385  
386  
387  
388  
389  
390  
391  
392  
393  
394  
395  
396  
397  
398  
399  
400  
401  
402  
403  
404  
405  
406  
407  
408  
409  
410  
411

- [1] Leonidas Guibas et.al Angel X. Chang, Thomas Funkhouser. Shapenet: An information-rich 3d model repository. In *Eu-  
rographics Workshop on 3D Object Retrieval*, 2015. 2, 3
- [2] Zhenwei Bian Jun Li-Kai Xu Chengjie Niu, Yang Yu. Weakly supervised part-wise 3d shape reconstruction from single-view rgb images. In *Computer Graphics Forum*, 2020. 2
- [3] Christopher B. Choy, Danfei Xu, JunYoung Gwak, Kevin Chen, and Silvio Savarese. 3d-r2n2: A unified approach for single and multi-view 3d object reconstruction. In *European Conference on Computer Vision (ECCV)*, 2016. 1, 2
- [4] Thibault Groueix, Matthew Fisher, Vladimir G. Kim, Bryan C. Russell, and Mathieu Aubry. Atlasnet: A papier-mâché approach to learning 3d surface generation. In *IEEE Conference on Computer Vision and Pattern Recognition (CVPR)*, 2018. 1
- [5] Leonidas Guibas Haoqiang Fan, Hao Su. A point set generation network for 3d object reconstruction from a single image. In *IEEE Conference on Computer Vision and Pattern Recognition (CVPR)*, 2017. 1, 2
- [6] Yiming Gao Xintao Wang-Shenghua Gao Ying Shan Jiale Xu, Weihao Cheng. Instantmesh: Efficient 3d mesh generation from a single image with sparse-view large reconstruction models. In *IEEE Conference on Computer Vision and Pattern Recognition (CVPR)*, 2024. 2, 5
- [7] Florian Golemo Jérôme Parent-Lévesque David Vazquez Derek Nowrouzezahrai Aaron Courville Sai Rajeswar, Fahim Mannan. Pix2shape: Towards unsupervised learning of 3d scenes from images using a view-based representation. In *International Journal of Computer Vision*, 2020. 2
- [8] Keke He Junwei Zhu-Ying Tai Chengjie Wang Yinda Zhang Yanwei Fu Shijie Zhang, Boyan Jiang. T-pixel2mesh: Combining global and local transformer for 3d mesh generation from a single image. In *IEEE International Conference on Acoustics, Speech and Signal Processing (ICASSP)*, 2024. 5
- [9] Maxim Tatarchenko, Alexey Dosovitskiy, and Thomas Brox. Octree generating networks: Efficient convolutional architectures for high-resolution 3d outputs. In *IEEE International Conference on Computer Vision (ICCV)*, 2017. 1
- [10] Nanyang Wang, Yinda Zhang, Zhuwen Li, Yanwei Fu, Wei Liu, and Yu-Gang Jiang. Pixel2mesh: Generating 3d mesh models from single rgb images. In *European Conference on Computer Vision (ECCV)*, 2018. 1, 2